WAVE-INDUCED SHIP MOTIONS IN HARBOUR ENTRANCES - A FIELD STUDY

by

A C van Wyk*

ABSTRACT

Extensive field monitoring programmes were implemented to study the behaviour of deep-draught ships in the entrance channels to two major South African ports. These programmes form part of a study to assess the future accessibility of these ports to ships of greater draught.

This paper describes briefly the monitoring techniques and methods of data analysis used, and reviews the results with regard to the environmental conditions during the monitoring operations.

The prototype results on ship response to waves will provide valuable data for the calibration and validation of both mathematical and physical models. The results are also used to establish allowance criteria based on safe underkeel allowances for ships presently using these harbours.

1. INTRODUCTION

In 1978 the Ship Dynamics Division of the National Research Institute for Oceanology started an extensive study, on behalf of the South African Transport Services, to determine criteria for optimum use by deep-draught ships of the entrance channels to the two major South African export harbours under adverse sea conditions.

The coal harbour at Richards Bay on the east coast presently handles bulk carriers of up to 150 000 dwt (17 m draught in an outer channel depth of -24,0 m CD (Chart Datum)) while the ore harbour at Saldanha Bay on the west coast frequently accommodates vessels of up to 270 000 dwt (21 m draught in an outer channel depth of -23,7 m CD).

---

* Ship Dynamics Division, National Research Institute for Oceanology, Council for Scientific and Industrial Research, Stellenbosch, RSA

Safe use of the entrances with respect to underkeel allowance during adverse sea conditions has become a matter of considerable importance in the light of demands for handling larger ships and of the high costs involved in deepening the channels.

As part of the overall study, field monitoring programmes were implemented at these harbours to record the behaviour of the larger ships using the entrance channels under various environmental conditions. The data are needed to calibrate and validate the mathematical and physical models to be used in future studies and, also to update the provisional allowance criteria used at present which were based on limited results of earlier model studies.

This paper describes briefly the monitoring techniques and methods of data analysis (covered in detail by Zwamborn and Van Wyk, 1981) and reviews the results with regard to the wave conditions during the monitoring operations. Since the emphasis is entirely on wave-induced vertical motions, horizontal behaviour of the ship is considered only in order to determine the direction of wave approach relative to the ship.

2. FIELD MONITORING

Ship behaviour is recorded by a method of discrete time-interval photography. The monitoring technique, basically, comprises taking photographs, from a land-based station, at 2 s intervals, of each ship during her transit of the entrance channel. The photographic equipment consists of a motorized 35 mm camera fitted with a telephoto lens which enables behaviour of the ship to be monitored over a distance of roughly 2 km in the channel. Recording is therefore limited to daylight hours and when visibility is satisfactory.

The environmental conditions recorded during each event comprise the wind, the tide and, particularly, the waves. A waverider system provides, during monitoring, a continuous record of the waves in the vicinity of the entrance channel while the dominant wave direction is obtained from clinometer observations, radar wave images or pilot boat observations.

Each ship is also visited after arrival or before departure to obtain essential geometric details of the ship as well as the loading condition at the time of sailing.

Since August 1978 just over 200 different shipping events have been monitored, about 90 per cent of them at Richards Bay. These events were rated according to the severity of the wave climate as well as quality and extent of the records.

3. DATA PROCESSING AND ANALYSIS

3.1 Film Processing

To date the photographic records of the 70 top-rated events (all of which were recorded at Richards Bay) have been processed using a simple photogrammetric technique. The procedure consists of digitizing target points on the images of the ship on each film negative relative to a fixed coordinate system.

These coordinates, together with the geometry of the ship, are used to compute:

(i) the vertical motions of the target points on, and

(ii) the route, heading and speed of each ship.

The motions of the target points are used to derive:

(a) the three principal motions, namely, roll, pitch and heave, and

(b) the vertical wave-induced motions at the perpendiculars, shoulders and quarters of the ship due to roll, pitch and heave.

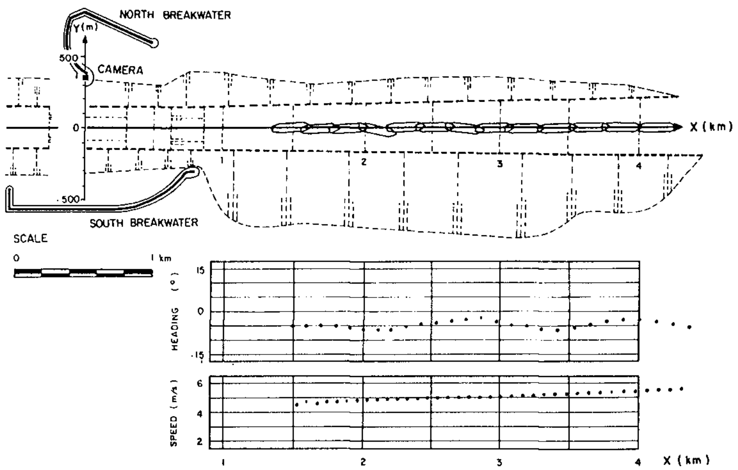

Figure 1.1 Ship trajectory for event R065

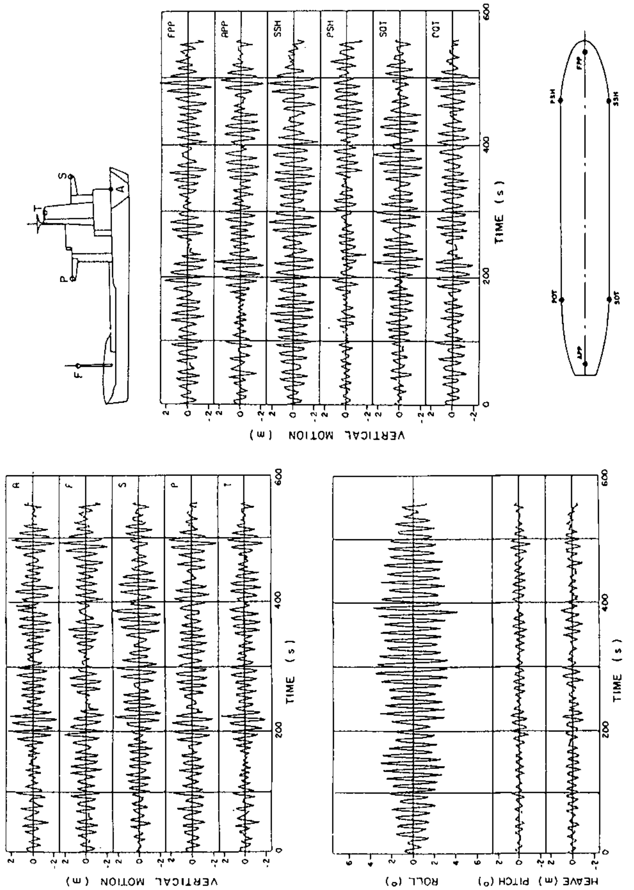

Figure 1.2 Sample motion time series for event R065

Examples of the results for a typical case study (event R065) are shown in Figures 1.1 and 1.2. Ship positioning relative to the channel coordinate system is believed to be accurate to within 50 m longitudinal and 10 m transverse. Heading angles relative to the channel orientation are accurate to about 1,5° and the speed of the ship averaged over intervals of 14 s is accurate to about 0,05 m/s. The vertical motions are subject to random measuring errors of about 0,1 m to 0,3 m depending on the distance from the camera to the ship (1 000 m to 3 000 m).

Since certain target points, particularly those chosen on the bow of departing ships, were frequently obscured from view, all three principal motions, and, consequently, the combined motions at the perpendiculars and shoulders of the ships, could not always be calculated. For the majority of the events the motions of only the port and starboard tips of the bridge superstructure and the stern of the departing ship could be obtained. The bridge motions, however, could be taken as approximately those of the ship's quarters since the bridge tips more or less coincide with the hull quarter points, the bridge width being equal to the beam of the ship.

3.2 Probabilistic Analysis

The motion time series, being, on average, of about 8 min duration, were accepted to be representative samples of a stationary random process so that the standard deviation of motion, s, could be used to characterise each record.

Normalized distributions of motion amplitude were derived for the motions at each target point and were compared with the well-known Rayleigh distribution given by

$$P(a) = \exp\left(-{}^1/_2\left(\frac{a}{s}\right)^2\right) \qquad \ldots\ 1$$

where a is the apparent amplitude of motion.

The calculated distributions were found to fit the Rayleigh distribution very well as is shown, for example, by the exceedence distribution of motion amplitudes at the port quarters of 70 different ships in Figure 2.

Longuet-Higgins (1952) postulated that the expected maximum amplitude, $E\{a_{max}\}$, in a given sample record with known standard deviation, s, and with Rayleigh-distributed apparent amplitudes, depends only on the record duration (number of oscillations, N) and is found from the relationship

$$E\{a_{max}\}/s = 2\left[(\ln N)^{1/2} + {}^1/_2\,\nu(\ln N)^{-1/2}\right] \qquad \ldots\ 2$$

with $\nu = 0{,}5772$ (Euler's constant).

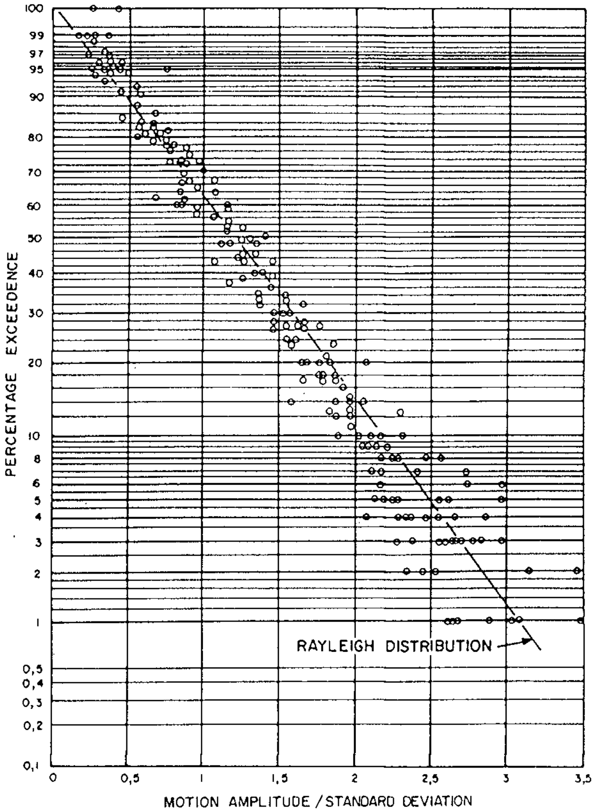

Figure 2 Distribution of motion amplitudes at port quarter

Using Equation 2, expected maximum motion amplitudes were calculated for 35 different records of from 20 to 50 oscillations and were compared with the recorded maxima as shown in Figure 3. Since Equation 2 apparently predicts the maximum motion amplitude well even for records of short length, this approach was adopted to estimate maxima from the sample standard deviations of motion and assuming that on average the ship underwent 100 oscillations for the period that she remained in the channel. Equation 2 then becomes

$$E\{a_{max}\} = 3{,}22\ s \qquad \ldots\ 3$$

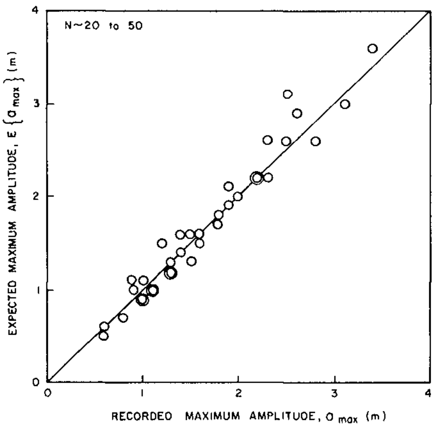

Figure 3 Expected versus recorded maximum motion amplitudes

3.3 Frequency Domain Analysis

For a selected number of events the incident wave records and ship motion records were spectrally analysed using a frequency resolution of 0,005 Hz.

The incident wave spectrum, S(f), was transformed to an apparent wave spectrum, $S_e(f_e)$ the wave spectrum encountered by the ship, using the relationships

$$S_e\ (f_e) = S(f)\ \frac{df}{df_e} \qquad \text{... 4a}$$

and

$$f_e = f - \frac{V}{\lambda}\cos\alpha \qquad \text{... 4b}$$

where V is the ship's speed, λ is the incident wavelength and α is the angle of wave incidence relative to the ship.

The incident and apparent wave spectra for event R065 are shown in Figure 4. The incident waves show a typical 1,7 m swell peaking at 15,4 s. With the dominant angle of wave incidence of 220° and taking the average speed of the ship to be 5 m/s (the ship in fact increased speed from 4,3 m/s to 5,5 m/s over a distance of roughly 2 km) the ship would have encountered the peak of the swell at about 12,2 s.

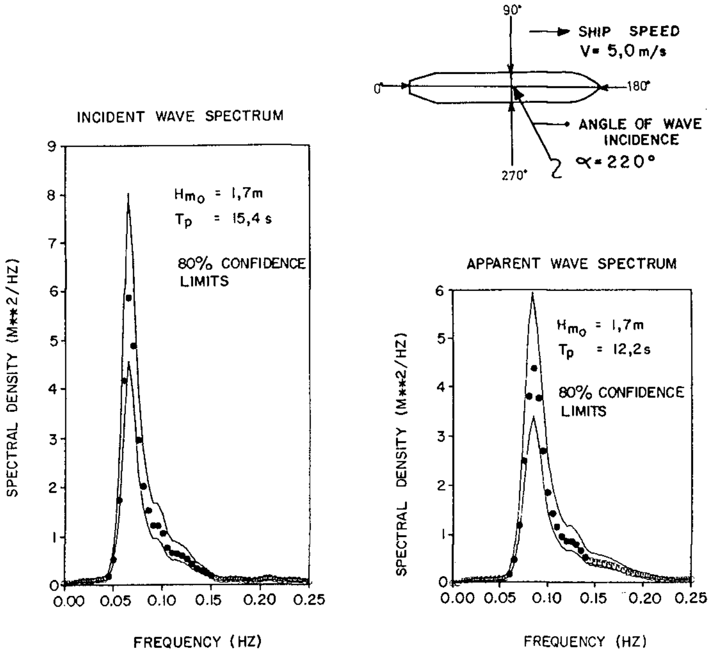

Figure 4 Incident and apparent wave spectra for event R065

Figure 5 illustrates the motion spectra of the ship, $S_s(f_e)$, for roll, pitch and heave and the combined motions were converted to translatory vertical motions at the ship's quarters.

From the assumption that a ship can be regarded as a linear system, the amplitude response function, $R(f_e)$, for each of the motions was calculated using the relationship

$$R(f_e) = \left[S_s(f_e)/S_e(f_e)\right]^{1/2} \qquad \ldots 5$$

The amplitude response functions for roll, pitch and heave and for the combined vertical motions at the quarters for the ship monitored during event R065 are shown in Figure 6.

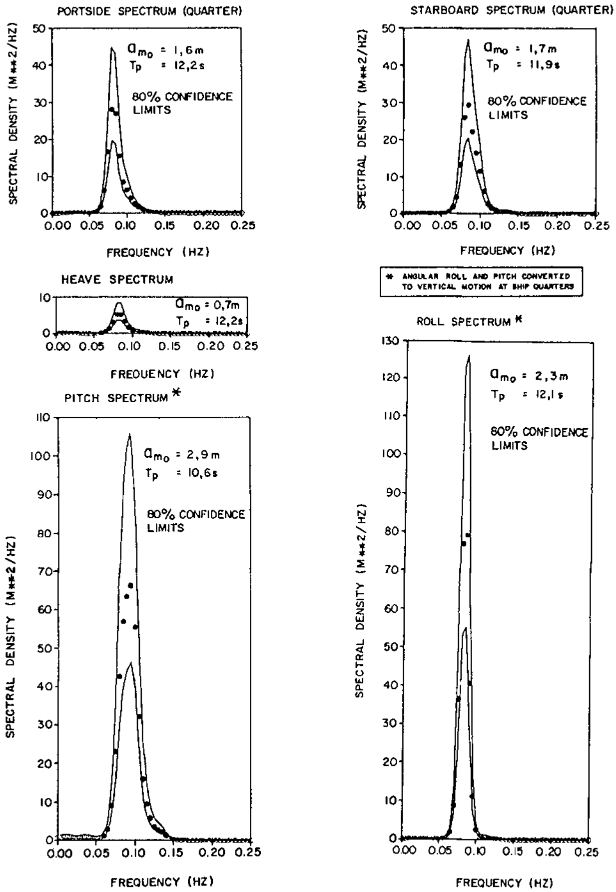

Figure 5 Sample ship motion spectra for event R065

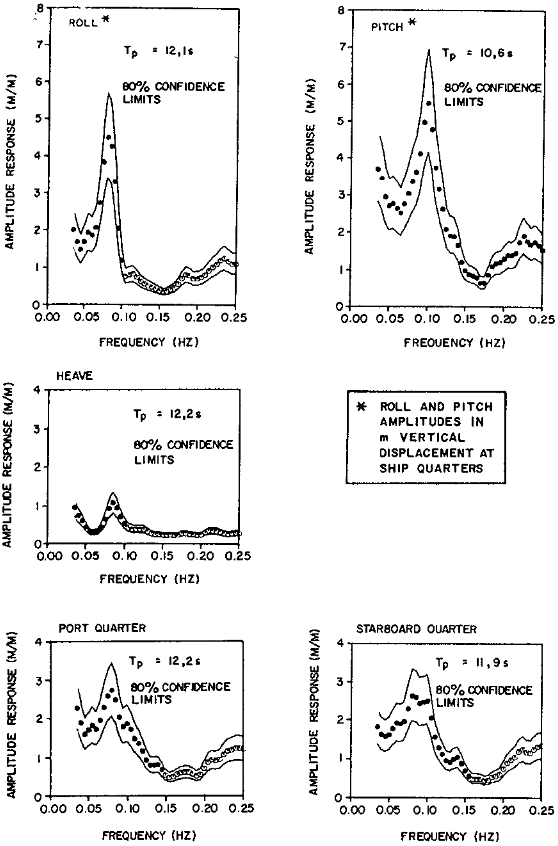

Figure 6 Sample amplitude response functions for event R065

4. DISCUSSION AND INTERPRETATION OF RESULTS

4.1 Maximum Ship Motions Versus Significant Wave Height

The expected maximum motion amplitudes calculated from the records with the largest standard deviations for each of the 70 processed events are shown plotted against significant wave height, H_{m_O} in Figure 7. The 18 events labelled with run numbers all took place under particularly adverse wave conditions.

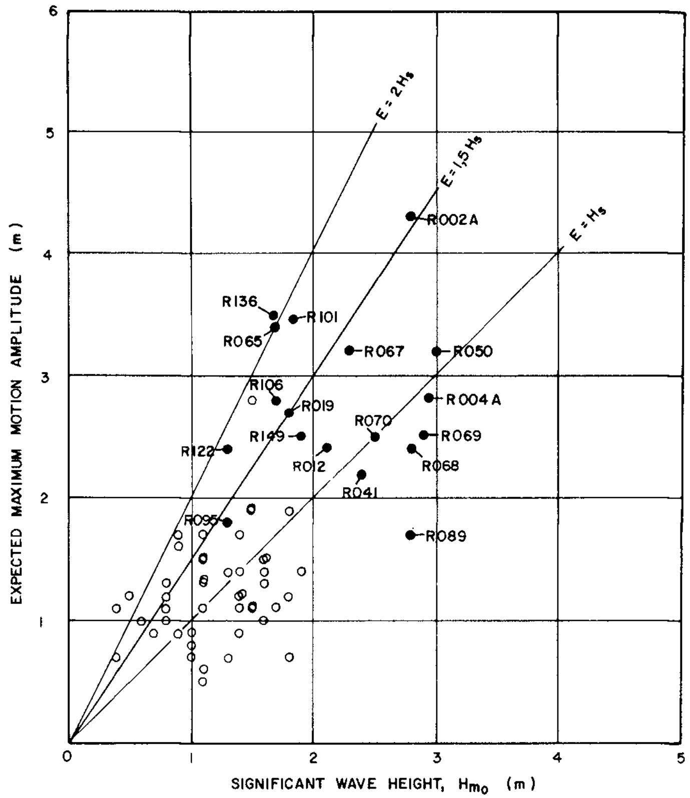

Figure 7 Maximum motion amplitude versus significant wave height

Gradients of 1:1, 3:2 and 2:1 were included showing that about 24 per cent of the data falls above the 3:2 gradient with significant wave heights generally less than 2 m. For larger wave heights the data always remained below the 3:2 gradient.

Inspection of the data enables the large variation in ship response to be attributed to a number of possible causes:

(i) **Variability of incident wave fields:** The wave spectra showed various stages of wind-generated seas and swells and were often composed of both. Swells approaching the channel varied in direction by as much as 70° and peaked at periods ranging from 11 s to well over 16 s. Heavy seas resulting from strong local winds were either beam-on or parallel to the channel line of orientation. The wind fields were, at times, of sufficient duration and strength to generate appreciable wave energy at periods of up to 12 s.

(ii) **Variations in ship's speed and heading:** Speeds ranged between 3 m/s (6 kn) and 6 m/s (12 kn) while ships, on leaving port, often increased speed by about 1 m/s to 2 m/s over a distance of 2 km. Angles of wave incidence relative to the ship also varied considerably due to variations in the ship's course. Figure 8 summarizes ship speed and angle of wave incidence for the 70 events considered in Figure 7.

(iii) **Differences in ship geometry and size:** The ships ranged in size from 95 000 dwt to 160 000 dwt and showed large variations in principal dimensions even for ships of equal displacement. Lengths between perpendiculars ranged from 240 m to 290 m and beams ranged from 37 m to 45 m.

(iv) **Differences in ship loading:** Ships leaving port were carrying from 100 000 t to just over 150 000 t of coal and had draughts ranging from 14 m to just over 17 m. The occasional entering ship was either in ballast or partly loaded.

Table I summarizes the principal ship dimensions and loading conditions for 18 of the 70 events (those numbered in Figure 7).

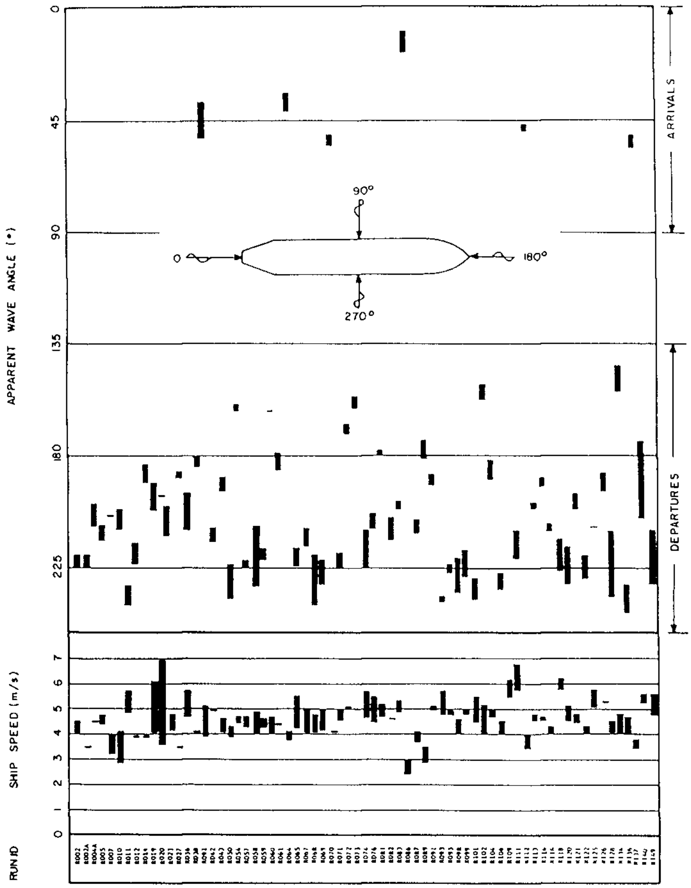

Figure 8 Range of apparent wave angles and ship speeds

TABLE I: SHIP PARTICULARS

Event	Ship code	Principal dimensions						Loading conditions						
		LOA (m)	LPP (m)	BEAM (m)	DRAFT (m)	LSW (t)	DWT (t)	Drafts (m) FWD	MID	AFT	DWT (t)	XG (m)	KG (m)	GM (m)
R002A	F(I)	260,0	248,0	41,6	16,81	19 819	125 103	16,55	16,80	16,61	123 125			
R004A	PP	259,8	249,0	39,6	15,78	20 180	112 731	15,36		15,83	109 437			
R012	NN	261,0	250,0	40,8	16,20	20 181	119 500	14,82	15,30	15,68	109 336			
R019	Q(II)	283,3	270,0	42,5	16,42	22 942	140 440	15,60	16,14	16,46	136 434	6,7	12,9	4,7
R041	V	250,1	237,0	38,9	14,68	20 189	95 357	9,14	9,94	10,74	42 208	-7,3	13,5	3,7
R050	F(I)	260,0	248,0	41,6	16,81	19 819	125 103	16,53	16,81	16,83	124 796	-5,8	10,7	6,1
R065	C(II)	266,0	251,5	38,4	15,78	19 910	110 338	15,39		15,93	110 318	1,9	8,1	7,5
R067	Q(II)	283,3	270,0	42,5	16,42	22 942	140 440	15,72	16,08	16,28	120 000	6,5	12,8	4,7
R068	OO	269,0	256,0	42,7	16,77	20 488	139 720	15,19	15,56	15,83	120 000			
R069	U(II)	303,0	287,0	43,0	16,64	28 854	148 200	16,26	16,59	16,15	144 964		13,1	4,5
R070	R(I)	261,0	247,0	40,6	17,61	20 739	129 629	12,30	12,50	12,80	74 000			
R089	E	292,0	280,4	42,7	17,30	24 276	154 483	17,06	17,06	17,06	152 267	2,5	12,7	4,9
R095	LL	268,0	259,0	39,0	16,08	18 407	123 000	15,70	16,00	16,00	122 800	-1,4	12,4	3,9
R101	EE(II)	261,0	249,0	39,6	16,45	20 407	118 712	15,39	15,77	16,08	112 210	5,8	12,2	3,7
R106	T	262,0	247,0	40,8	17,58	23 525	129 537	17,07		17,09	122 045	7,1	8,8	7,7
R122	MM	280,0	266,5	43,4	16,61		153 322	16,23		16,84	133 081	7,3		
R136	E	292,0	280,4	42,7	17,30	24 276	154 483	17,25	17,15	17,22	147 863			
R149	PP(I)	267,6	259,0	39,0	16,09	18 311	123 125	13,90	14,30	14,70				

4.2 Hull Points of Maximum Vertical Motion

The wave-induced vertical motions at the perpendiculars, shoulders and quarters of the ships could be calculated from the measured target motions for 25 of the 70 processed events.

For these events expected maximum motion amplitudes at both starboard shoulders and starboard quarters (thus, on the weather side of the ship) were, at times, up to about 50 per cent larger than the motions at their port-side counterparts (Figures 9a and b). A comparison of the starboard motions at the quarters and shoulders of these ships (Figure 9c), however, showed no tendency for motions at one point to be consistently larger than those at the other point.

Motions at the forward perpendiculars (resulting purely from heave and pitch), moreover, were of the same order of magnitude as those at the shoulders and quarters (which also include roll), Figure 9d. This emphasizes the fact that, in the majority of cases, wave encounter was such as to also stimulate ship motions in the pitch mode.

4.3 Ship Response Functions

Ship response functions were calculated from the motion spectra and wave spectra for the 18 events identified in Figure 7. The ship particulars are listed in Table I and the wave and ship response data are summarized in Table II.

Observations of dominant wave directions were often limited to visual clinometer measurements only and could, sometimes, be very misleading, particularly with strong winds which caused very confused sea states. Thus, verification of the primary wave fields was obtained by relating incident wave spectra to meteorological conditions prior to and during these events. The synoptic weather charts were found to be useful for delineating the primary sources of wave generation and to confirm the deep-sea swell directions. These were then converted to wave directions in and around the channel by means of appropriate refraction diagrams, and the results were checked against the local observations.

The extreme swells recorded during these events can be seen to have propagated from three primary directions, these being SSW/SW'ly, S'ly and SSE'ly. The peak swell periods ranged from 11,7 s to as long as 17,8 s and significant wave heights ranged from 1,2 m to 3,0 m.

These swells were refracted considerably while approaching the channel because of the coastal bathymetry and this

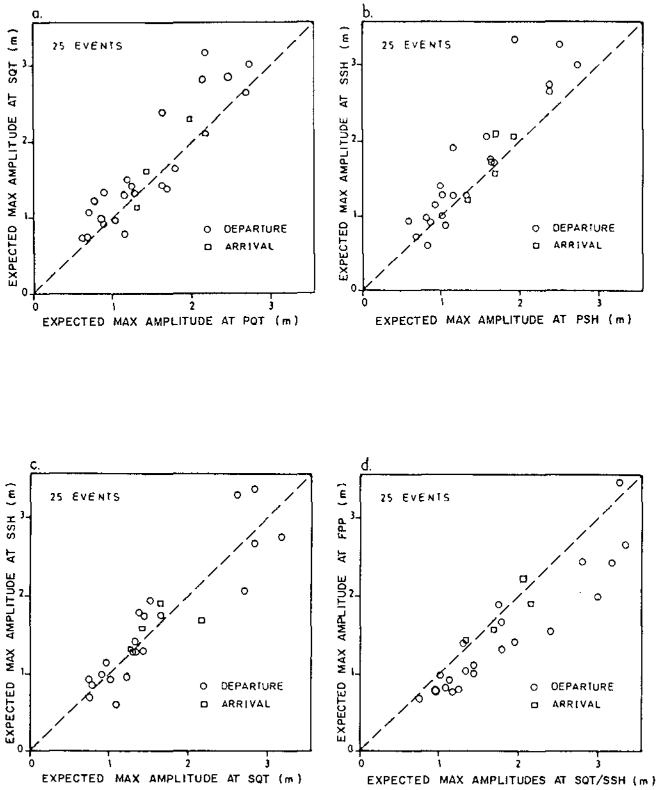

Figure 9 Hull motion relationships

TABLE II: WAVE AND SHIP RESPONSE DATA

Event	Incident waves				Ship/wave encounter				Ship response									
									Roll		Pitch		Heave		P.qrt		Stb.qrt	
	H_{mo} (m)	T_p (s)	θ_o	$\theta_{channel}$	D/A*	V (m/s)	α (°)	T_e (s)	T_p (s)	R_{max} (m/m)	T_p (s)	R_{max} (m/m)	T_p (s)	R_{max} (m/m)	T_p (s)	R_{max} (m/m)	T_p (s)	R_{max} (m/m)
R002A	2,7	14,5	SSW/S	140→150	D	3,5	210	12,0	12,2	3,5	11,9		12,1		12,2	2,3	11,8	2,0
R004A	2,7	17,8	SSW	135→155	D	4,5	220→210	14,5→14,0	13,0	2,0					13,4	1,6	13,3	1,4
R012	1,8	12,5	SW/SSW	150→160	D	3,9	215→225	10,0→10,5	11,1	3,4					11,3	2,0	11,0	2,0
R019	1,8	11,7	S	145→155	D	4,1→6,1	215→220	9,5→9,0	11,2	3,3	11,4		11,3		11,5	2,5	11,1	2,3
R041	2,4	14,1 (8,0)	SW/SSW (SE)	145→155 (130→135)	A	3,9→5,1	35 (15→20)	18,0→19,5 (12,0→13,5)	11,5	0,6	14,9 (10,2)				13,6 (17,0)	1,5	11,8	1,0
R050	3,0	15,4	SW/SSW	140→155	D	3,9→4,2	190→210	12,5	12,0	4,0					12,5	2,6	11,5	2,8
R065	1,7	15,4	SW/SSW	140→155	D	4,3→5,5	215→230	12,5→13	12,1	4,5	10,6	5,5	12,1	1,0	12,5	2,6	11,9	2,6
R067	2,3	14,3	S	140→150	D	4,1→5,0	210→225	11,5	11,7	2,5	10,7	3,5	12,2		12,1	1,0	10,9	2,0
R068	2,8	12,5	S	145→155	D	4,1→4,8	205→220	10,0	11,1	2,4					11,1	1,5	10,1	1,7
R069	3,0	14,2	SSE	135→140	D	5,0→4,2	205	10,5→11,5	11,0	1,0	11,1		11,1		11,1	0,9	11,1	0,6
R070	2,6	14,2	SSE	135→140	A	4,1	35→25	18,5	12,2	2,0	15,4		14,7 (19,0)		15,1	1,0	15,4 (12,3)	1,0
R089	2,8	11,7	SSW/S	145→160	D	2,9→2,5	220→225	10,0→10,5	11,5	2,7					10,6	1,3	11,1	2,3
R095	1,2	13,2	S	145→150	D	4,8	215→220	10,5	11,0	4,5	10,1	3,0	11,1	0,7	11,0	3,1	10,8	2,3
R101	1,7	15,5	SW/SSW	140→155	D	4,5→5,5	210→220	12,5→12,0	11,8	4,0					12,1	2,7	11,6	2,8
R106	1,7	13,4	SW	150→160	D	4,1→4,5	215→235	11,0→11,5	12,2	4,4	11,0	7,0	11,2	0,8	12,0	2,4	11,2	3,0
R122	1,4	13,0 (11,0)	SW/SSW (S/SSE)	150→160 (145→150)	D	4,3→4,0	215→220	10,5 (9,0)	11,4	5,3					11,8	2,6	11,2	3,9
R136	1,6	13,8	SW/SSW	145→160	D	4,7→4,1	220→225	11,0→11,5	11,8	2,7	11,9		12,1		12,2	2,8	11,4	2,6
R149A	1,8	13,8	SSW	145→155	D	4,8→5,6	195→220	10,5	10,5	4,0					10,7	2,6	10,5	2,6

* D - departure
A - arrival

resulted in channel wave directions being confined to a narrower sector ranging from 130° to 160° TN.

When allowance was made for the ship's heading relative to the channel orientation, the angles of wave incidence to the ships while leaving port ranged from about 190° to 235° (bow waves) and depended both on the directions and periods of the swells. The periods of wave encounter thus were shorter than those of the incident waves. Both ships entering port (events R041 and R070) encountered quartering waves with the resultant periods of wave encounter being much longer than those of the incident waves.

The motion amplitude response functions for the ships are characterised by the maximum amplitude response and corresponding period in Table II.

Maximum response ranged between 2,5 and 5,3 for roll at periods of wave encounter between 11 s and 12 s. Pitch and heave response could be assessed only for a limited number of these ships. Pitch resonance seemed to occur at periods between 10 s and 11 s. Maximum response factors at these periods were usually large, a value of 7 having been recorded at one occasion. Heave response, however, showed little, if any, gain at the normal periods of wave encounter.

Maximum amplitude response at the port and starboard quarters of the ships showed values of up to 4, but generally remained below 3.

Motion amplitude response due to combined roll, pitch and heave motions were much less than would have resulted from simply adding the contributions algebraically. This indicates strong phase dependence between the three principal motions.

5. CONCLUSIONS

The field monitoring programmes have been successful in providing useful data on wave-induced vertical ship motions as well as on ship speeds and ship trajectories under a variety of wave conditions.

The data, particularly the amplitude response functions, will prove valuable for the calibration of both mathematical and physical models which are presently being developed and which will be deployed to assess harbour accessibility for future deeper-draught ships. The measurements are also useful in verifying and updating existing allowance criteria based on limited earlier model tests.

Since vertical wave-induced ship motions are intrinsically narrow-banded and amplitudes are found to be Rayleigh-distributed, maxima can be estimated well by means of the Longuet-Higgins approach.

Though plots of expected maximum motion amplitude versus significant wave height showed large variations due to differences in both the wave conditions and ship characteristics, maximum amplitudes were shown to **never exceed twice the significant wave height** in magnitude.

Starboard motions were frequently **larger** than port side motions while motions at the perpendiculars of the ships were often of the same order of magnitude. It became evident that both pitch and roll contributed largely to the vertical hull motions while a strong phase dependence exists between all three principal motions.

The longer period swells (14 s to 16 s) proved to be most critical with regard to vertical ship motions for ships leaving port since these ships tended to encounter the waves at periods close to their natural resonance periods. These swells, however, would have less effect on ships entering port since the periods of wave encounter would then be far removed from their own natural periods of oscillation.

Acknowledgements

The author is grateful to the South African Transport Services for their permission to publish this paper.

REFERENCES

ZWAMBORN, J A and VAN WYK, A C (1981). Monitoring of ship motions in the Richards Bay harbour entrance channel. Proceedings of the XXVth International Navigation Congress, PIANC, Edinburgh.

LONGUET-HIGGINS, M S (1952). On the statistical distribution of the heights of sea waves. Jnl. of Marine Research, Vol XI, No 3.